

## Article

# Constructing a Model of *Populus* spp. Growth Rate Based on the Model Fusion and Analysis of Its Growth Rate Differences and Distribution Characteristics under Different Classes of Environmental Indicators

Biao Zhang <sup>1,†</sup> , Guowei Liu <sup>2,†</sup>, Zhongke Feng <sup>1,\*</sup> , Mingjuan Zhang <sup>1</sup>, Tiantian Ma <sup>1</sup>, Xin Zhao <sup>3</sup>, Zhiqiang Su <sup>3</sup>  and Xiaoyuan Zhang <sup>3,\*</sup>

<sup>1</sup> Precision Forestry Key Laboratory of Beijing, Beijing Forestry University, Tsinghua East Road, Beijing 100083, China

<sup>2</sup> Henan Province Forestry Resources Monitoring Institute, Zhengzhou 450045, China

<sup>3</sup> College of Materials Science and Engineering, Beijing University of Chemical Technology, Beijing 100029, China

\* Correspondence: zhongkefeng@bjfu.edu.cn (Z.F.); xiaoyuan.zhang@buct.edu.cn (X.Z.)

† These authors contributed equally to this work.

**Abstract:** Poplar (*Populus* spp.) is an important forest species widely distributed in China of great significance in identifying factors that clearly influence its growth rate in order to achieve effective control of poplar growth. In this study, we selected 16 factors, including tree size, competition, climate, location, topography, and soil characteristics, to construct linear regression (LR), multilayer perceptron (MLP), k-nearest neighbor regression (KNN), gradient boosting decision tree (GBDT), extreme gradient boosting (XGB), random forest (RF), and deep neural network (DNN) models based on the poplar growth rate. Using model fusion methods, the fitting accuracy and estimation capability were improved. The relative importance of each variable in estimating the poplar growth rate was analyzed using the permutation importance evaluation. The results showed the following: (1) the model fusion approach significantly improved the estimation accuracy of the poplar growth rate model with an  $R^2$  of 0.893; (2) the temperature and precipitation exhibited the highest importance in poplar growth; (3) the forest stand density, precipitation, elevation, and temperature had significant variations in growth rates among different-sized poplar trees within different ranges; (4) low-forest stand density, high-precipitation, low-elevation, and high-temperature environments significantly increased the poplar growth rate and had a larger proportion of large-sized individuals with high growth rates. In conclusion, environmental factors significantly influence poplar growth, and corresponding planting and protection measures should be tailored to different growth environments to effectively enhance the growth of poplar plantations.

**Keywords:** machine learning; poplar growth rate; environmental factors; model fusion; size variations; plantation management measures



**Citation:** Zhang, B.; Liu, G.; Feng, Z.; Zhang, M.; Ma, T.; Zhao, X.; Su, Z.; Zhang, X. Constructing a Model of *Populus* spp. Growth Rate Based on the Model Fusion and Analysis of Its Growth Rate Differences and Distribution Characteristics under Different Classes of Environmental Indicators. *Forests* **2023**, *14*, 2073. <https://doi.org/10.3390/f14102073>

Academic Editor: Nikolay Strigul

Received: 5 September 2023

Revised: 29 September 2023

Accepted: 10 October 2023

Published: 17 October 2023



**Copyright:** © 2023 by the authors. Licensee MDPI, Basel, Switzerland. This article is an open access article distributed under the terms and conditions of the Creative Commons Attribution (CC BY) license (<https://creativecommons.org/licenses/by/4.0/>).

## 1. Introduction

Poplar trees (*Populus* spp.) are recognized for their rapid growth, ease of reproduction, strong adaptability, and short rotation period. They are the most widely cultivated broad-leaved tree species in China [1,2]. According to the Ninth China Forest Resources Inventory Report (2019), poplar plantation forests covered an area of 7,570,700 hectares, with a storage volume of 546 million cubic meters. In addition, poplar ranked second in planted tree forests, accounting for 13.25% of the total planted forest area and 16.12% of the total stock volume. The results can be attributed to, among other things, rapid growth characteristics and active reforestation efforts. These efforts have been important in alleviating short-term timber shortages [3].

In the establishment of artificial poplar forests, certain regions face challenges, including slowed growth, reduced biodiversity, and soil degradation due to climate change, poor forest resource management, and unsuitable environments. Within the Three-North Shelter Forest Program, over 4 million hectares are covered by artificial poplar forests, receiving substantial resources for cultivation. However, poplar trees demand abundant water, straining limited resources and leading to degraded conditions. The forest structure lacks proper design, with excessive pure poplar forests and insufficient mixed forests. “Old small-headed trees” covering 1.4 million hectares are proliferating, along with pest infestations, destabilizing ecosystems [4]. The Loess Plateau prioritizes trees over shrubs and grass, violating vegetation rules and promoting “small old trees”. In Zhangjiakou, a key poplar shelter forest has degraded significantly, with 4/5 of the area affected, leading to stunted growth and reduced protective function [5].

Unfavorable site conditions, low precipitation, and erosion limit growth in many artificial poplar forests [6,7]. Scarce soil moisture and nutrients hinder tree nourishment, aggravated by inadequate pruning practices. This degradation influences tree growth and the forest’s surroundings.

In recent decades, extensive research has been conducted by scholars on the mechanisms of how site conditions and environmental factors impact tree growth and the development of growth models for poplar trees. The response of tree growth to climate is influenced by various factors, including tree size [8], age [9], stand structure [10,11], and soil characteristics [12,13]. Variations in these factors can lead to differences in the way poplar trees respond to climate. For instance, temperature, precipitation, and light have been identified as important influencing factors [14]. Studies have observed that high temperatures and drought have inhibitory effects on poplar tree growth [5,15], while favorable temperature and moisture conditions promote growth. Additionally, researchers have investigated the effects of soil texture, nutrient content, and moisture conditions on tree growth [12]. The correlations between poplar growth and climate variables at monthly, seasonal, and annual scales have also been explored, highlighting the strongest and most consistent associations with precipitation, which is crucial for site water balance [16]. Moreover, elevation has been identified as a factor that influences poplar growth, as trees in high-altitude areas adapt to the plateau climate by adjusting their growth rate and lifespan [17]. The interactions among climate, site conditions, and competition can impact the growth of individual trees within a population, and this effect may vary depending on species and size [18]. While climate has a direct influence on tree growth, management practices like nitrogen fertilization, irrigation, logging strategies, and planting density can also interact with climate and further impact tree growth [19]. Therefore, when studying forest growth and related subjects, it is crucial to consider the variations arising from changes in these environmental factors [20].

Forest growth models are valuable tools used to forecast and simulate the structure, function, and growth of forest ecosystems [21]. These models can be utilized at different levels of resolution, including stand, cohort, and individual tree levels [22]. Nevertheless, stand and cohort-level growth models are limited in accurately representing the intricate and fine-scale variations within forest ecosystems, such as accounting for individual differences, addressing spatial heterogeneity, and capturing complex interaction relationships. In contrast, individual tree growth models provide greater flexibility and can effectively depict the growth dynamics of mixed and uneven-aged stands with heterogeneous and structurally complex attributes [23].

In the realm of research on individual tree growth models, scholars have employed diverse research methodologies. Traditional growth models predominantly rely on statistical and mathematical approaches, such as linear regression and empirical models [24–27]. Recently, tree growth models rooted in machine learning algorithms have garnered considerable attention [18,28,29]. These algorithms, encompassing random forests and neural networks, possess the capability to enhance the accurate prediction of tree growth processes. In order to augment predictive performance and robustness, fusion methods for models have been implemented in the forestry domain [30,31]. Despite the widespread utilization

of methods like ensemble learning and hybrid models in other domains, their application for estimating forest growth remains relatively limited.

However, despite the substantial progress made in studying the environmental factors that promote tree growth, there remain unresolved issues that necessitate further research. Although various growth models have been utilized in previous studies for prediction purposes, conventional statistical methods and mathematical models still possess certain limitations. Typically based on linear relationships or assumptions of specific functional forms, these models are incapable of capturing intricate nonlinear relationships and variations. Consequently, it is imperative to leverage advanced machine learning algorithms and model fusion techniques to enhance the prediction accuracy and generalization capability of poplar growth models. Furthermore, existing research on the influence of environmental factors on poplar growth fails to consider their impact on the growth and development of poplars of different sizes. Understanding the growth patterns of varying-sized poplars under distinct environmental factors is fundamental in effectively evaluating and designing optimal areas for poplar tree cultivation. Therefore, it is crucial to delve deeper into the mechanisms and dynamic changes associated with the influence of environmental factors on poplar growth.

This study investigates the influence and distribution characteristics of these factors on the growth rate of poplar trees across different ranges by employing a model fusion-based multi-factor analysis method. The study workflow consists of three main steps: (1) Establishing a growth rate model for poplar trees using model fusion. A model is developed by considering multiple factors, such as geographic environment, climate, and competition within the stand, with the aim of predicting the growth rate of poplar trees and improving prediction accuracy and stability. (2) Creating an optimal growth rate model based on model fusion. The relative contributions of environmental factors are assessed and ranked using the Permutation Importance method. (3) Selecting four indicators—stand density, precipitation, altitude, and temperature—as the key features and dividing them into five levels. This study explores the variations in the growth rate of poplar trees across different levels of each indicator. (4) Investigating the distribution characteristics of the growth rate of poplar trees under different levels of indicators to unveil the extent and patterns of their influence. Through a comprehensive analysis of the integrated effects of environmental factors at different levels on poplar tree growth, this study provides valuable insights for assessing and managing poplar growth rates.

## 2. Materials and Methods

### 2.1. Study Site

The People's Republic of China encompasses six distinct climatic regions: tropical (including the entirety of Hainan province and the southern regions of Yunnan, Guangdong, and Taiwan), subtropical (south of the Qinling–Huaihe River and east of the Qinghai–Tibet Plateau), warm temperate (encompassing major areas in the middle and lower reaches of the Yellow River and southern Xinjiang), temperate (Northeast China, most of Inner Mongolia, and the northern parts of Xinjiang), cold temperate (northern Heilongjiang Province and northeastern Inner Mongolia), and plateau (Qinghai–Tibet Plateau region).

The tropical climate zone is characterized by warm and humid conditions with plentiful annual rainfall. The predominant vegetation in this zone is tropical rainforests, which consist of towering trees, vines, clustered plants, and aquatic vegetation. The subtropical climatic region experiences distinct seasons, featuring mild winters and hot, humid summers, with relatively evenly distributed rainfall. The primary vegetation types in this region include coniferous forests, broadleaf forests, bamboo forests, and grasslands. The temperate climate zone is characterized by cold and dry conditions, with extended, harsh winters and brief, cool summers. The primary vegetation types in this zone include grasslands, coniferous forests, deciduous broadleaf forests, and desertified areas. The subarctic climate zone experiences cold and arid conditions characterized by lengthy, harsh winters and brief, cool summers. The prevailing vegetation types in this zone consist of

coniferous forests and tundra, with tundra being predominantly found in high-altitude areas. The plateau climate zone exhibits cold and arid conditions characterized by considerable temperature fluctuations with altitude. The primary vegetation types in this zone comprise alpine meadows, shrublands, and tundra. Additionally, the low-lying areas also contain grasslands and coniferous forests to some extent.

## 2.2. Data Collection and Feature Selection

The National Forest Inventory (NFI) is conducted to comprehensively assess the status and dynamic changes of forest resources, with the goal of providing an objective reflection of forest quantity, quality, structure, and functionality. The NFI employs fixed sample plots for regularly repeated surveys [3]. Our study utilized NFI data from 7801 permanent plots predominantly populated by poplar trees (Figure 1). The data spans the years 1999–2003, 2004–2008, 2009–2013, and 2014–2018. The survey data comprises over 27,000 poplar trees, covering a latitude range of 23.9° N to 53.5° N and a longitude range of 76.0° E to 133.8° E. The elevation varies from 0 to 4110 m, the annual average precipitation ranges from 36.6 mm to 2461.4 mm, and the annual average temperature spans from  $-4.5$  °C to 23.48 °C. For each plot, forest stand factors such as individual tree diameter at breast height (DBH, cm), mean diameter at breast height of the plot (SMDBH, cm), stand density (DENS, trees/ha), and basal area ( $m^2$ /ha) were subjected to statistical analysis. Additionally, the analysis incorporated site factors such as longitude (B, °), latitude (L, °), elevation (ELEV, m), slope (SLOPE, °), aspect (ASPECT, °), slope position (SP), and soil thickness (ST, cm). Slope, slope age, and slope position are considered virtual variables. The slope orientation (AP) is classified into eight categories: flat/north-facing (AP\_1), northeast-facing (AP\_2), east-facing (AP\_3), southeast-facing (AP\_4), south-facing (AP\_5), west-facing (AP\_6), southwest-facing (AP\_7), and northwest-facing (AP\_8). The age class (AC) is categorized into five subclasses: young forest (AC\_1), middle-aged forest (AC\_2), near-mature forest (AC\_3), mature forest (AC\_4), and over-mature forest (AC\_5). The slope position (SP) is classified into six specific locations: ridge (SP\_1), upper slope (SP\_2), middle slope (SP\_3), lower slope (SP\_4), valley (SP\_5), and flat terrain (SP\_6).

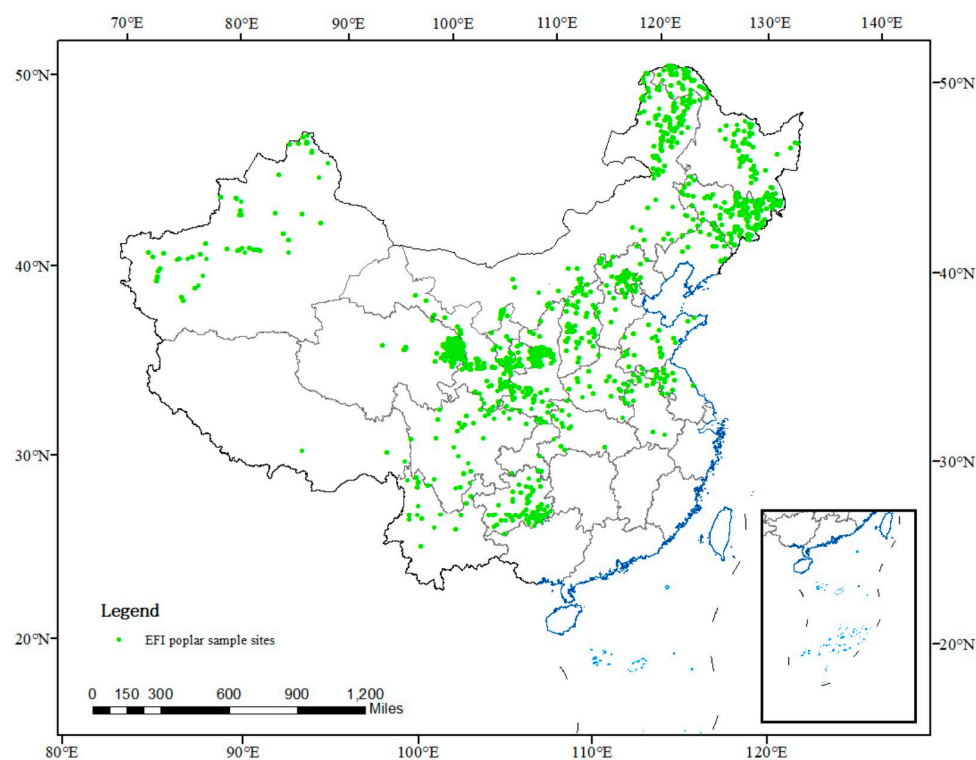


Figure 1. Distribution of EFI poplar sample sites.

The ClimateAP software (Version 2.30, <https://asiapacific.forestry.ubc.ca/research-approaches/climate-modeling/>, accessed on 9 October 2023) can generate site-specific, unscaled climate data for historical years and time periods. In version 2.30, the historical time range has been extended from 1901–2017 to 1901–2019 [32–34]. As the positioning of EFI for sample plots relies on point location data, we utilized the ClimateAP program to investigate the influence of climate variables on poplar tree DBH in China. We utilized spatial interpolation estimation of historical climate data to obtain the geographical attributes for each sampling point. Four climate variables, namely mean annual temperature (MAT), mean annual precipitation (MAP), mean warmest month temperature (MWTM), and mean coldest month temperature (MCMT), were chosen as candidate independent variables to calibrate the tree growth model. To account for the variation in survey periods among provinces, we filtered the meteorological data for each province based on their respective survey periods and utilized the average values as the meteorological indicators for each sampling site.

Finally, 16 features were incorporated as crucial factors for modeling poplar tree growth, encompassing MAT, MAP, AC, DBH, SMDBH, DENS, BAL, ELEV, SLOPE, ST, ASPECT, MWTM, MCMT, B, L, and SP. These factors encompass the dimensions of individual trees, competition, climate, location, topography, and soil, constituting the six feature categories. Various indicators are employed to measure tree growth, such as the diameter increment at breast height between two survey periods ( $\Delta\text{DBH} = \text{DBH}_2 - \text{DBH}_1$ ), the ratio of diameter increment to the diameter value at the previous survey period ( $\Delta\text{DBH}/\text{DBH}_1$ ), the squared diameter increment ( $\text{DDS} = \text{DBH}_2^2 - \text{DBH}_1^2$ ), and the logarithmic value of the squared diameter increment plus a constant 1 ( $\ln(\text{DDS} + 1)$ ). Site productivity in this study was evaluated based on the diameter growth rate, which reflects the growth condition of poplar trees influenced by various modeling factors [35]. The overall technology path is depicted (Figure 2).

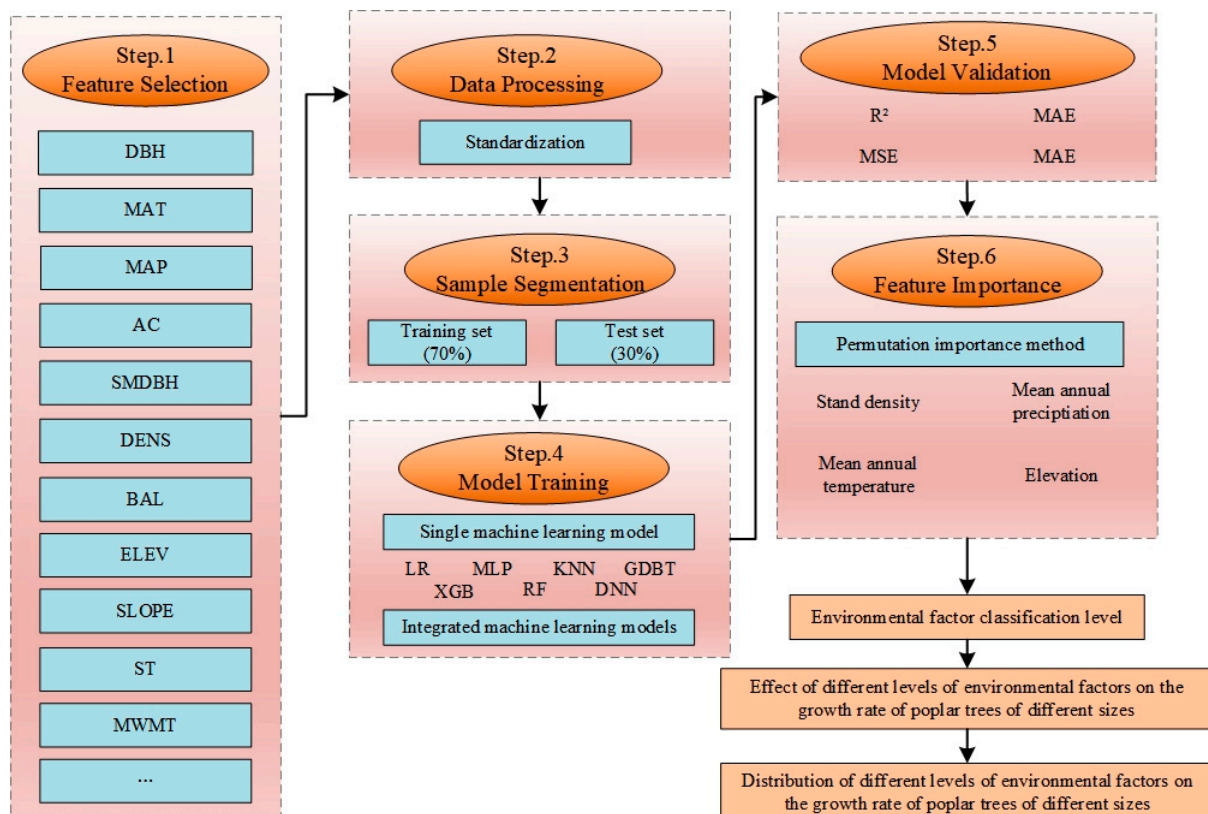


Figure 2. Technology roadmap for this study.

### 2.3. Model Construction

Linear regression is a statistical method utilized to establish a linear relationship model among variables. Model coefficients are determined by minimizing the sum of squared residuals using the least squares method [36]. Linear regression offers advantages stemming from its simplicity, efficiency, and strong interpretability. However, it performs inadequately in modeling nonlinear relationships, is sensitive to assumptions about data distribution and feature correlation, and is highly influenced by outliers.

Multilayer Perceptron (MLP) is a commonly employed feedforward neural network model for regression problems [37]. This model acquires and represents intricate nonlinear relationships through nonlinear computations within multiple neural layers. MLP is suitable for processing large-scale datasets, but it necessitates meticulous parameter initialization and hyperparameter selection. The training process demands substantial amounts of data and computational resources.

K-nearest neighbor regression is a non-parametric regression algorithm that predicts the target variable's value by identifying the K nearest neighbors to the test sample within the training dataset [38,39]. This method does not rely on any specific data distribution and is well suited for addressing nonlinear relationships. However, it exhibits high computational complexity and is subject to sensitivity based on the choice of the K value.

The Gradient Boosting Decision Tree (GBDT) regression model is an ensemble learning method that iteratively constructs decision tree models and optimizes the loss function using gradient descent for regression tasks [40]. The Extreme Gradient Boosting (XGBoost) regression model is an optimized algorithm based on Gradient Boosting Decision Tree, utilized for regression problems [40].

Extreme Gradient Boosting (XGBoost) regression model is an optimized algorithm based on Gradient Boosting Decision Tree used for regression problems [40]. Its advantages lie in the high efficiency and accuracy, but careful tuning of hyperparameters is required, and it is sensitive to the scale of training data.

The Random Forest (RF) regression model is an ensemble learning method that constructs multiple decision trees through random sampling and feature selection. The final prediction is obtained by averaging or voting the predictions of these trees [41,42]. Its strengths lie in its strong robustness, but it may not perform well on data with many redundant features, and the results are less interpretable.

The Deep Neural Network (DNN) is a neural network model with multiple hidden layers designed to handle large-scale data and complex problems [43]. This method can learn complex non-linear relationships, but it requires longer training time and is sensitive to parameter initialization and hyperparameter selection.

In this study, the LR, MLP, KNN, GBDT, XGBoost, RF, and DNN models were constructed using the Sklearn and Pytorch packages in Python. The GridSearchCV package was applied to search for the optimal hyperparameter configurations [44,45]. Based on the establishment of these seven models, model fusion was utilized to optimize the fitting accuracy and enhance the prediction capabilities in terms of accuracy and robustness. For regression problems, model fusion is a technique that combines the predictions of multiple base models using weighted averaging to produce the results. Common fusion methods include simple averaging, weighted averaging, and voting. In this study, the predictions of multiple base models were used as new features for training the meta-model. The meta-model used in this study was LR, and the optimal combination of base models was selected using a grid search algorithm to effectively leverage the strengths of different models and enhance the overall performance.

### 2.4. Feature Relative Importance Assessment

The Permutation Importance evaluation method is a widely employed statistical technique for selecting features and assessing their importance. It measures feature importance by randomly permuting them and comparing changes in the model's performance [46]. The fundamental principle is to disrupt the relationship between features and the target variable

by altering the order of feature values. The contribution of each feature to the model's performance is then assessed. When a feature has a noteworthy impact on the model's performance, permuting its values will lead to a noticeable decrease in performance. The process of the Permutation Importance evaluation method involves constructing a baseline model and recording its performance metrics. Next, the values of each feature are randomly permuted while keeping other features unchanged, and the model's performance metrics are recalculated. By comparing the model's performance after each feature permutation with the baseline model, the importance scores of each feature are obtained. Based on the importance score, one can decide whether to retain features with greater importance or conduct further analysis of their impact. The calculation process is shown in Equation (1):

$$Importance(f_j) = \frac{1}{N} \sum_{i=1}^N [Loss(y_i, \hat{y}_i) - Loss(y_i, \hat{y}_i^{(j)})] \quad (1)$$

where  $Importance(f_j)$  represents the importance of the  $j$ th feature.  $Metric$  is the loss function used to evaluate the model's prediction error.  $y_i$  denotes the true value,  $\hat{y}_i$  represents the original model's predicted value, and  $\hat{y}_i^{(j)}$  indicates the model's predicted value after randomly reordering the  $j$ th feature.

### 2.5. Environmental Factor Feature Grading

To evaluate the impact of stand density, rainfall, elevation, and temperature on the growth of various-sized poplar trees, we categorized these four indicators into five levels using a uniform distribution approach (Table 1).

**Table 1.** Environmental factors classification standard.

Class	DENS (Plants/ha)	MAP (mm)	ELEV (m)	MAT (°C)
Low	16–939	42.6–322.0	0–500	−4.5–0
Mid-Low	940–1859	322.1–638.2	500–1500	0–5
Mid	1860–2779	638.3–954.4	1500–2500	5–10
Mid-High	2780–3699	954.5–1360.6	2500–3500	10–15
High	3700–4633	1360.7–2387.6	3500–4163	15–25

Note: The table presents associations between the 5 classes and the combinations of DENS, MAP, ELEV, and MAT. For example, the range of 16–939 for DENS corresponds to the density range of the Low Class, while the range between 638.3–954.4 mm for MAP represents the rainfall range of the Mid Class.

### 2.6. Model Evaluation

In this study, we utilized the following approaches to validate and assess the constructed regression model. We standardized the input data to maintain a consistent scale across different features. Standardization is accomplished by subtracting the mean from each data point and dividing by the standard deviation. The aim of this procedure is to minimize feature variations, enabling the model to effectively capture the relationships among them. The calculation process is shown in Equation (2):

$$x_{norm} = \frac{x - x_{min}}{x_{max} - x_{min}} \quad (2)$$

where  $x_{norm}$ ,  $x$ ,  $x_{min}$ , and  $x_{max}$  represent the normalized, original, minimum, and maximum values from the training data.

Subsequently, we assess the performance of the regression model using three widely employed metrics: Mean Absolute Error (MAE), Root Mean Squared Error (RMSE), and Coefficient of Determination ( $R^2$ ). The formulas are Equation (1), Equation (2), Equation (3), respectively:

$$MAE = \frac{1}{n} \times \sum_{i=1}^n |y_i - \hat{y}_i| \quad (3)$$

$$RMSE = \sqrt{\frac{\sum_{i=1}^n (y_i - \hat{y}_i)^2}{n}} \quad (4)$$

$$R^2 = 1 - \frac{\sum_{i=1}^n (y_i - \hat{y}_i)^2}{\sum_{i=1}^n (y_i - \bar{y})^2} \quad (5)$$

where  $n$ ,  $y_i$ , and  $\hat{y}_i$  represent the number of data sets, measured values, and predicted values, respectively.

For model validation, we partitioned the dataset into separate training and test sets. During the training phase, we utilized the training set to train the model and optimize its parameters by minimizing the loss function. During the testing phase, we evaluated the model's performance by utilizing the test set and computing metrics, including MAE, RMSE, and  $R^2$ .

### 3. Results

#### 3.1. Comparison of Multiple Growth Rate Models

The accuracy validation results of the eight models are presented (Figure 3 and Table 2). The LR and MLP models exhibited relatively higher MAE and RMSE values: 3.194% and 4.081%, 3.697% and 4.840%, respectively. Conversely, the KNN model showed relatively lower MAE and RMSE values: 3.009% and 3.869%. While the RMSE values of the GDBT and XGB models were comparable, the GDBT model had a slightly higher MAE value at 4.092% compared to 3.691% for the XGB model. In contrast, the KNN model exhibited comparatively lower MAE and RMSE values at 3.009% and 3.869%, respectively. The GDBT and XGB models had similar RMSE values, while the GDBT model had a slightly higher MAE value at 4.092% compared to 3.691% for the XGB model. The RF model yielded MAE and RMSE values of 3.462% and 4.706%, whereas the DNN model demonstrated lower values of MAE and RMSE at 2.492% and 3.467%, respectively. Overall, the DNN-RF combined model showcased the best performance, achieving MAE and RMSE values of 1.958% and 2.844%, respectively, along with an  $R^2$  of 0.893. Consequently, the DNN-RF combined model excels in prediction capability and stability while also compensating for errors from both models, thereby enhancing accuracy.

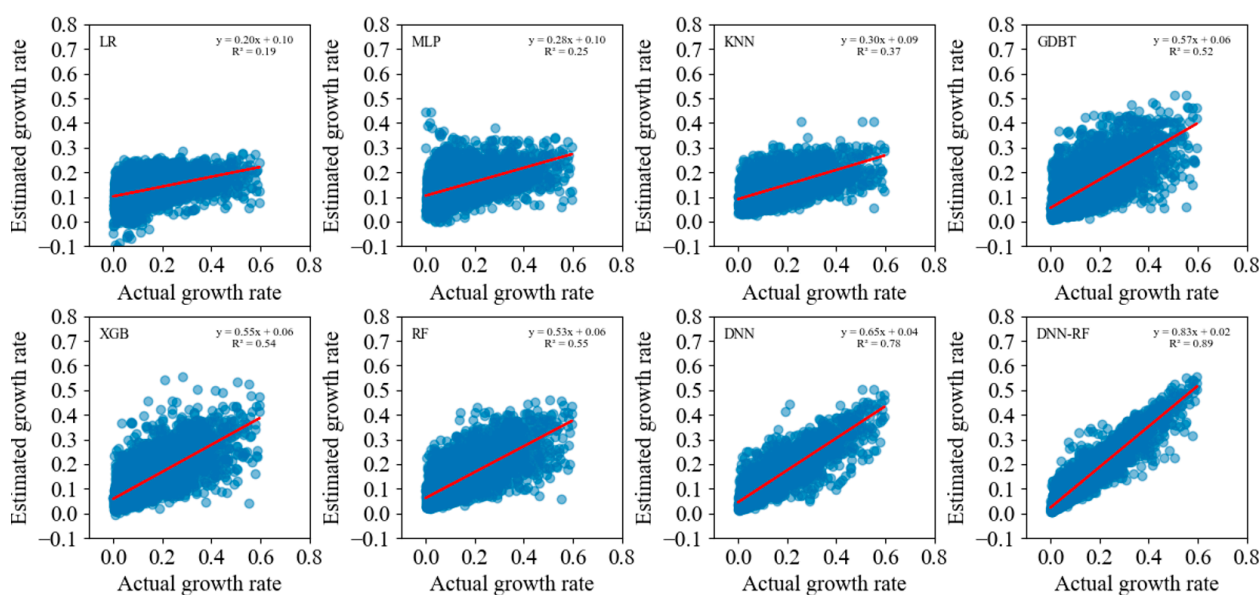


**Figure 3.** Scatter plot depicting the fitting of eight models for estimating the growth rate of poplar's diameter at breast height.

**Table 2.** Comparative analysis of MAE, RMSE, and R<sup>2</sup> for assessing the accuracy of DBH growth rate models.

Model	DBH Growth Rate			DBH Growth Amount			Prediction of the Next Period's DBH		
	MAE/%	RMSE/%	R <sup>2</sup>	MAE/cm	RMSE/cm	R <sup>2</sup>	MAE/cm	RMSE/cm	R <sup>2</sup>
LR	3.194%	4.081%	0.192	0.537	0.747	0.329	0.852	1.208	0.974
MLP	3.697%	4.840%	0.254	0.635	0.971	0.347	0.825	1.243	0.975
KNN	3.009%	3.869%	0.370	0.512	0.737	0.448	0.752	1.105	0.979
GDBT	4.092%	5.558%	0.515	0.568	0.880	0.580	0.630	0.987	0.983
XGB	3.691%	5.042%	0.542	0.513	0.769	0.620	0.601	0.920	0.985
RF	3.462%	4.706%	0.554	0.500	0.758	0.619	0.598	0.918	0.986
DNN	2.492%	3.467%	0.778	0.343	0.516	0.816	0.423	0.652	0.993
DNN-RF	1.958%	2.844%	0.893	0.249	0.372	0.924	0.269	0.416	0.997

### 3.2. Relative Importance Assessment of Optimal Models

We conducted a quantitative assessment of the importance of 16 features in the estimation of poplar growth rate using the permutation importance method (Figure 4). The results revealed that mean annual temperature (MAT) had the highest relative importance among all features, with a value of 0.485, indicating a strong influence on the growth rate of poplar. The importance score of mean annual precipitation (MAP) was 0.417, indicating a significant impact of precipitation conditions on poplar growth. Concerning age groups, the total importance score was 0.26. In our model, the age class (AC) was divided into five stages: young forest (AC\_1), middle-aged forest (AC\_2), near-mature forest (AC\_3), mature forest (AC\_4), and over-mature forest (AC\_5). Middle-aged forest (AC\_2) had the highest importance score of 0.083 among these stages, followed by young forest (AC\_1) with a score of 0.076. Near-mature forest (AC\_3) had an importance score of 0.069. In contrast, mature forest (AC\_4) and over-mature forest (AC\_5) had lower importance scores of 0.021 and 0.011, respectively. Regarding forest structure features, diameter at breast height (DBH), stand mean diameter at breast height (SMDBH), density (DENS), and basal area per unit area (BAL) achieved respective importance scores of 0.306, 0.284, 0.267, and 0.254, suggesting that these features have an impact on poplar growth. Regarding geographical and soil condition features, we found that elevation (ELEV), slope (SLPOE), and soil thickness (ST) had respective importance scores of 0.223, 0.178, and 0.167, suggesting that poplar growth may also be influenced to some degree by terrain and soil conditions. The overall importance score of the slope aspect (AP) feature is 0.139, demonstrating variations in the impact of each slope aspect on poplar growth. The south-facing slope (AP\_5) exerts the greatest influence on poplar growth, with an importance score of 0.033, indicating that the sunny south-facing slope may represent the most ideal location for poplar growth. Following them are the southeast-facing slope (AP\_4) and east-facing slope (AP\_3), with importance scores of 0.030 and 0.025, respectively. The impact of the flat or north-facing slope (AP\_1) on poplar growth is also significant, having an importance score of 0.019. The southwest-facing slope (AP\_7) and west-facing slope (AP\_6) exhibit lower importance scores of 0.015 and 0.009, respectively, suggesting that they may not be the preferred locations for poplar growth. Finally, the northeast-facing slope (AP\_2) and northwest-facing slope (AP\_8) have the lowest importance scores of 0.006 and 0.002, respectively. Additionally, we observed that the importance scores for the warmest month mean temperature (MWMT) and coldest month mean temperature (MCMT) are 0.111 and 0.092, respectively, which may reveal the impact of temperature range on poplar growth. Lastly, the importance scores for longitude (B), latitude (L), and slope position (SP) are relatively low, measuring at 0.081, 0.074, and 0.068, respectively. Among the six slope positions, the importance score of the downslope (SP\_4) is the highest, at 0.018. Next is valley (SP\_5) with a score of 0.016, followed by mid-slope (SP\_3) with a score of 0.014. Upslope (SP\_2), flat ground (SP\_6), and ridge (SP\_1) have lower importance scores of 0.009, 0.007, and 0.004, respectively. In comparison to the ridge, upslope, and flat ground, poplar growth is likely to be more influenced by mid-slope,

downslope, and valley positions. This observation suggests that the influence of these spatial and topographic features on poplar growth is relatively minor.

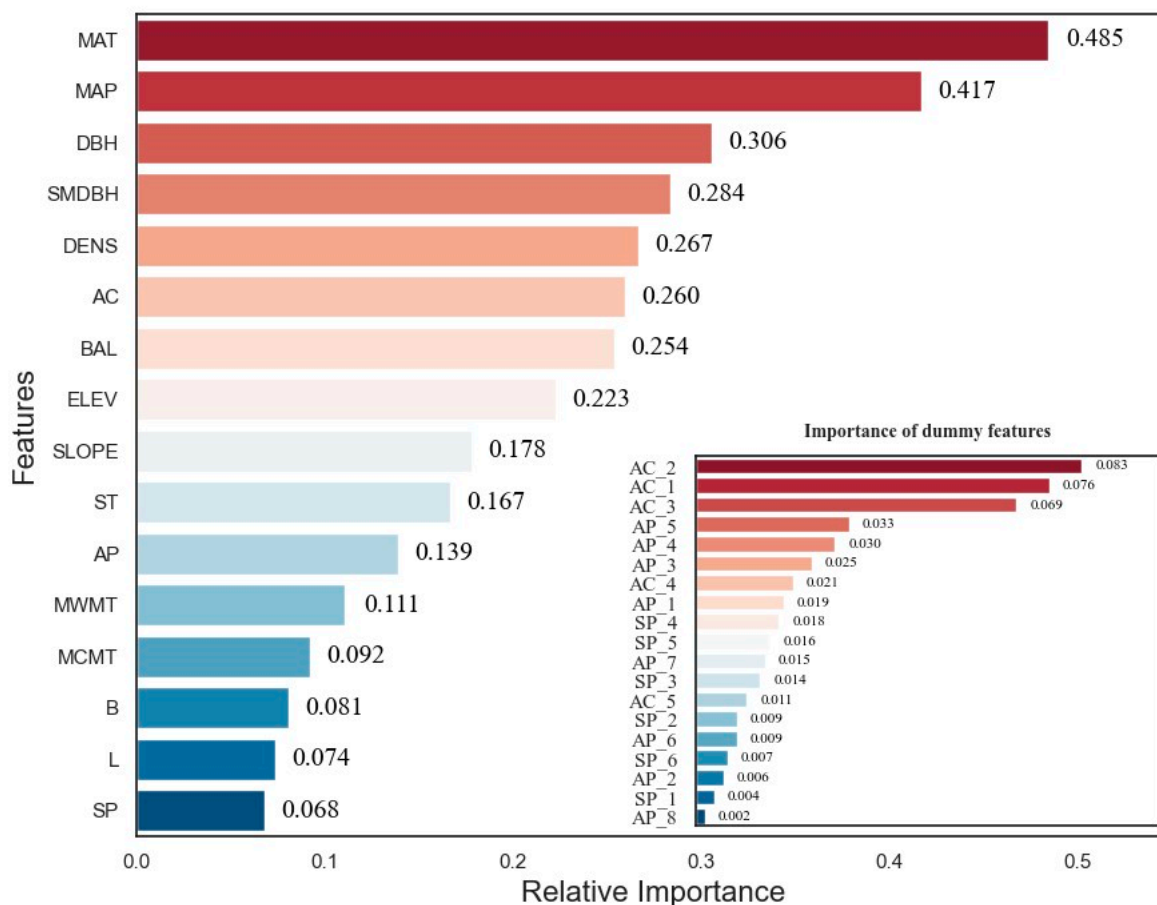


Figure 4. Feature relative importance assessment based on permutation method.

### 3.3. Analysis of Growth Rate Differences among Poplar Trees in Four Distinct Environmental Classes

The fitting analysis with the optimal model revealed distinct effects of stand density, precipitation, elevation, and temperature on the growth rate of poplar trees, as evident in the resulting curve (Figure 5). Significant variations in stand density, precipitation, elevation, and temperature were identified across different levels.

The growth rate of poplar trees decreases as tree size increases under low and medium-low stand densities, following the expected growth pattern. In contrast, medium-low stand density has a slightly weaker influence on growth rate compared to low stand density. Under medium stand density, poplar trees with a DBH of 5–20 cm exhibit lower growth rates than those with low and medium-low stand densities. Poplar trees with a DBH ranging from 20 to 35 cm display a stable growth rate, whereas trees with a DBH exceeding 35 cm experience a sharp decline in growth rate, reaching near-zero values at approximately 42.5 cm. Poplar trees with a DBH of 5–10 cm under medium-high stand density exhibit a consistent growth rate of approximately 0.1. In contrast, the growth rate of larger trees declines rapidly as the DBH increases, eventually approaching zero around 25 cm. In high stand density conditions, poplar trees with a DBH of 5–10 cm display a lower growth rate compared to other density levels, experiencing a gradual decline after 10 cm and reaching approximately 0.05 prior to reaching a DBH of 30 cm. Notably, poplar trees are scarce with a DBH exceeding 30 cm within this density level. Various density levels exert distinct effects on the growth rate, leading to significant fluctuations depending on the tree’s DBH. For instance, under medium-low stand density, poplar trees with a DBH larger than 30 cm,

those with a DBH ranging between 25 and 30 cm under medium stand density, those with a DBH around 15 cm under medium-high stand density, and those with a DBH around 10 cm under high stand density.

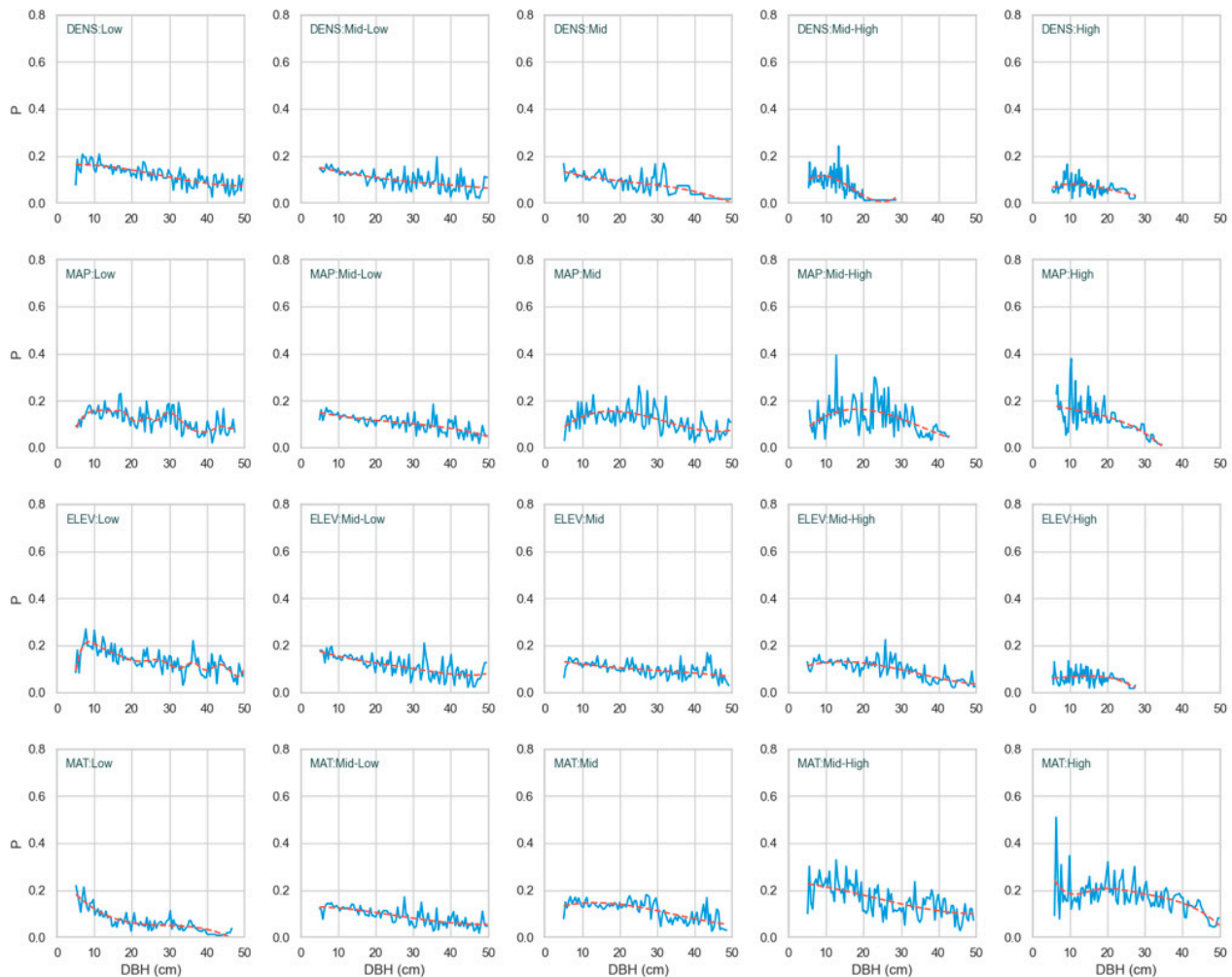


**Figure 5.** Variation in the impact of environmental factors at varying levels on the growth rate of poplars of different sizes (the blue curve represents the optimal model fit, while the red curve represents the smoothed curve).

The impact of various rainfall levels on poplar tree growth rate varies depending on their size. In low rainfall conditions, the growth rate of poplar trees experiences an increase between 5–10 cm, reaching its peak at 0.18 within the 10–15 cm range. Nevertheless, with increasing diameter at breast height (DBH), the growth rate of poplar trees exhibits fluctuations before reaching its minimum of 0.08 near 40 cm. When subjected to medium-low rainfall, the growth rate demonstrates a linear decline, decreasing from 0.15 at 5 cm DBH to approximately 0.05. The effect of moderate rainfall on the growth rate demonstrates a non-linear relationship. Among poplar trees with DBH ranging from 5 to 20 cm, the growth rate initially increases gradually from 0.1 to approximately 0.17. Subsequently, there is a rapid decline in growth rate, reaching its minimum around 45 cm DBH, exhibiting a decline similar to that observed at 5 cm DBH. The impact of medium-high rainfall similarly displays a non-linear fluctuation. For poplar trees with a DBH ranging from 5 to 20 cm, the growth rate gradually increases until peaking at 0.18, after which it steadily decreases with increasing DBH. In high rainfall conditions, the growth rate demonstrates a general decrease as the DBH increases. Notably, in low rainfall conditions, poplar trees with smaller DBH display higher growth rates, with the rate gradually decreasing from 0.2 at 5 cm

DBH to approximately 0.1 near 27.5 cm DBH, followed by a rapid decline. Moreover, we observed that higher rainfall levels resulted in more pronounced variations in the growth rate among poplar trees of different sizes, particularly within the range of 5–25 cm DBH under medium-high rainfall and the range of 5–15 cm DBH under high rainfall.

The growth rate of poplar trees exhibits significant variation across different elevations. With increasing elevation, the growth rate of poplar trees decreases gradually, irrespective of their size. At low elevations, the growth rate of poplar trees demonstrates a positive correlation with DBH. The growth rate reaches a peak value of 2.2 at a DBH of 8 cm and subsequently experiences fluctuations and a gradual decline but still maintains a minimum point above 0.1. The growth rate curves at medium-low and medium elevations exhibit a similar decreasing pattern. Once the DBH surpasses 50 cm, the growth rate decreases to approximately 0.8. The distinction lies in the initial point of the growth rate curve, which is 0.18 for medium-low elevation and 0.13 for medium elevation. In high-altitude environments, there is a consistent growth rate pattern for poplar trees with a DBH ranging from 5 to 15 cm, which remains around 0.13. However, the growth rate begins to decrease when the DBH surpasses this range. The growth rate curve remains lower in high-altitude environments. For poplar trees with a DBH between 5 and 20 cm, the growth rate hovers around 0.07 but declines rapidly beyond this range. Regarding growth rate fluctuations, poplar trees at lower altitudes exhibit more pronounced variations among different tree sizes. In medium-low-altitude environments, the growth rate of poplar trees shows fewer fluctuations within the 20 cm DBH range but demonstrates more pronounced variations beyond that threshold. In medium-altitude environments, the growth rate of poplar trees exhibits moderate fluctuations. In medium-high-altitude environments, there is significant fluctuation in the growth rate of poplar trees with DBHs around 25–30 cm. In high-altitude environments, poplar trees with a DBH below 20 cm show substantial growth rate fluctuations.

The analysis reveals that as temperature increases, each temperature curve positively influences the growth rate of poplar trees across different sizes. Furthermore, higher temperature curves consistently remain above their lower counterparts. With the increase in DBH, the growth rate of poplar trees in low-temperature environments gradually decreases. For instance, when the DBH is 5 cm, the initial growth rate is 0.2; it then rapidly decreases to approximately 0.04 and approaches 0 as the DBH reaches 45 cm. In contrast to low temperatures, the growth rate curves for medium-low and medium-level temperatures display smoother trends, particularly with increasing DBH, leading to a more gradual change in growth rate. Under medium-high temperature conditions, the growth rate of poplar trees at varying DBHs continues to increase, ranging from 0.23 for a 5 cm DBH to 0.1 for a 50 cm DBH, indicating a high growth rate. In high-temperature environments, smaller poplar trees experience a slight decline between 5 and 10 cm DBH but maintain a high growth rate ranging from 0.2 for a 10–25 cm DBH. Afterward, the decline becomes more pronounced, and at a DBH of 50 cm, the growth rate decreases to approximately 0.07. In medium-high and high-temperature conditions, the growth rates of poplar trees of different sizes display fluctuating patterns with increasing amplitude.

#### *3.4. Analysis of the Distribution of Poplar Growth Rates across Four Distinct Environmental Classes*

Using the scatterplot data, we generated a two-dimensional kernel density plot to examine how various levels of environmental factors affect the distribution of poplar tree DBH and growth rate (Figure 6). For brevity, we will focus solely on the darkest regions of the plot, indicating areas with the highest and greatest density. We have designated these areas as the relatively high-density distribution area of individual poplar trees (RHDDA) and the high-density distribution area (HDDA), respectively. These areas correspond to the first and second quartiles of the color gradient.

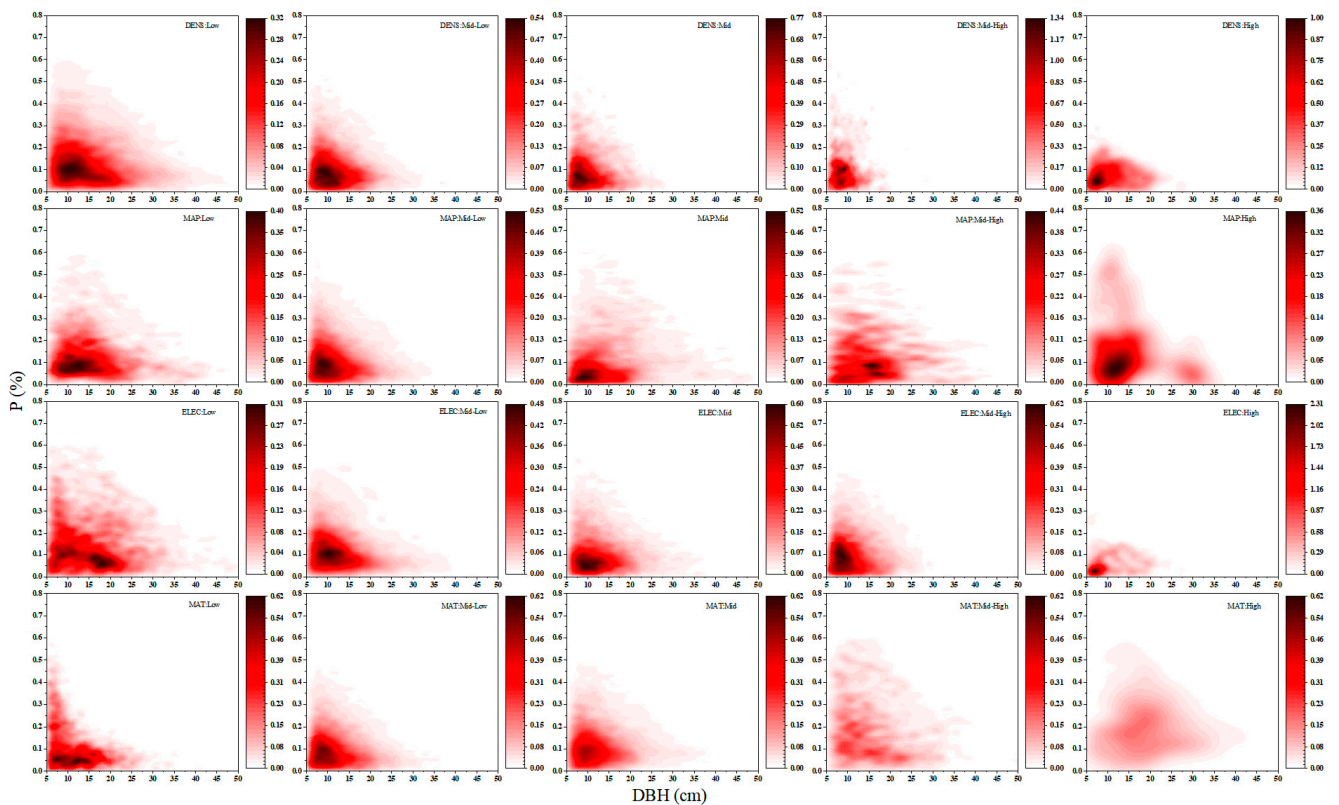


**Figure 6.** Differences in the distribution of different levels of environmental factors on the growth rate of poplar trees of different sizes.

As the density of poplar stands varies across a spectrum, ranging from low to high levels, the HDDA gradually diminishes towards the origin. This decrease suggests a greater prevalence of smaller-sized and slower-growing poplar trees, with individuals becoming more concentrated in the low-sized and low growth rate region. Conversely, the RHHDA also experiences a reduction in the area as it approaches the origin when transitioning from low to medium-high stand density environments. Moreover, under high stand density conditions, the RHHDA is uniformly distributed within the range of 5–20 cm trunk diameter and 0–0.2 growth rate. The effects of rainfall on the HDDA differ depending on the region. In areas with low rainfall levels, the HDDA is observed as a horizontally elongated region between trunk diameter sizes of 5–20 cm and growth rates of 0.5–1.5, whereas the RHHDA surrounds the region between trunk diameter sizes of 5–25 cm and growth rates of 0.025–0.2. In regions with medium-low rainfall, the vertical area of the HDDA expands, and the growth rate increases to around 0.15 vertically, while the RHHDA takes the form of a right-angled triangle with a trunk diameter range of 7.5–15 cm and a growth rate between 0.5–0.15 vertically. In regions with medium rainfall levels, both the vertical growth rates of the HDDA and RHHDA are further compressed towards the origin. In regions with medium-high rainfall levels, the horizontal shift of the HDDA is not accompanied by a corresponding increase in growth rate, thereby leading to the proliferation of high-sized poplar trees with low growth rates. The vertical expansion of the HDDA predominantly occurs in regions characterized by high rainfall levels, predominantly among individuals with trunk diameters ranging from 7.5 to 15 cm and growth rates between 0.15 and 0.25. Regarding regions with medium-high rainfall levels, the distribution of the RHHDA encompasses individuals with trunk diameters ranging from 5 to 25 cm and growth rates between 0 and 0.3. However, in regions with high rainfall levels, the distribution spans individuals with trunk diameters ranging from 5 to 30 cm and growth rates between 0 and 0.2. The distribution pattern of the HDDA and RHHDA is influenced by changes in elevation. With increasing elevation, both the HDDA

and RHDDA are influenced, progressively diminishing, and ultimately distributing within the narrower size range and lower growth rates characteristic of high-elevation regions. The HDDA exhibits an L-shaped pattern in cooler temperature regions, primarily concentrated between trunk diameters of 5–10 cm and vertical growth rates of 0–0.35, as well as between trunk diameters of 10–25 cm and horizontal growth rates of 0–0.1. As temperature rises, the territorial extent of the HDDA decreases. In regions with medium-high temperature levels, the HDDA eventually completely vanishes. Furthermore, as temperature continues to increase, the RHDDA gradually dwindles.

#### 4. Discussion

The growth of DBH presents a complex nonlinear phenomenon [47]. Various algorithms are employed in this study to address this issue. The results demonstrate that the DNN-RF-integrated algorithm leverages the capabilities of DNN in handling high-dimensional and nonlinear problems, as well as RF in addressing data with high variance and noise. The MAE was calculated as 1.958%, RMSE as 2.844%, and  $R^2$  as 0.893. Compared to the results obtained from a single machine learning model, the ensemble model exhibited superior predictive ability and stability, thereby enhancing the performance of the DBH growth rate prediction model.

The Permutation Importance scores obtained in our study revealed that stand density, rainfall, altitude, and temperature were significant factors influencing the growth rate of poplar trees. These findings align with the findings reported by others [48–50]. The subsequent examination of the effects of these factors on poplar growth unveiled notable discrepancies in how stand density, rainfall, altitude, and temperature at various levels influenced the growth rate of poplar trees across different sizes [51]. For ease of describing poplar growth, we classified the trees into three diameter ranges according to their breast diameters: small (5–15 cm), medium (15–30 cm), and large (exceeding 30 cm).

Forest stand density is negatively correlated with the growth of poplar trees. With an increase in the surrounding stand density, the growth rate of individual poplar trees decreases, similar to the findings of [52]. The results of this study reveal the influence of stand density on the growth rate of poplar trees of different diameter classes. In environments with low to moderate stand densities, the growth rate of poplar trees in the small diameter class remains relatively stable, whereas, in environments with moderate to high stand densities, their growth rate shows increased fluctuations. Likewise, medium-diameter class poplar trees show fewer fluctuations in growth rates in low stand density environments, but fluctuations increase in environments with moderate to low to moderate stand densities. The growth rate of large-diameter class poplar trees shows significant fluctuations in low to moderate to low stand density environments, but it gradually stabilizes in environments with moderate stand density. It is noteworthy that large-diameter class poplar trees struggle to survive in environments with moderate to high stand densities. These phenomena can be explained by theories of resource competition and environmental stress [53,54]. In low stand density environments, where there is abundant sunlight, soil moisture, and nutrient resources, there is less competition among trees. This leads to a positive growth response in small and medium diameter class poplar trees with low stand densities [55]. With an increase in stand density, resources become limited, intensifying competition among trees [56]. The growth rate of poplar trees in the small diameter class exhibits increased volatility, accompanied by individual variations in growth speed, which may be influenced by factors such as genetics, sprouting time, and location. The deceleration of growth rate in poplar trees of medium diameter class can be attributed to competition for resources and constraints in growth space. Concurrently, the population of poplar trees in the large diameter class gradually diminishes. In high-density stand environments, intense individual competition leads to stronger suppression of the growth rate in the large-diameter class of poplar trees, which demands additional resources to sustain growth. Consequently, with an increase in stand density, the growth rate of poplar trees in the small diameter class exhibits greater fluctuation, while the growth rate of trees in the medium diameter

class begins to decelerate, and the population of large diameter class trees gradually diminishes. Study [57] has demonstrated that reducing forest density can enhance the drought resistance of large trees. Furthermore, our study shows that reducing stand density has a positive impact on the growth of poplar trees in the small diameter class. Therefore, decreasing stand density via thinning, which enhances resource availability, is a viable approach to achieve the management objective of improving productivity [58,59].

The DBH growth of certain tree species is primarily controlled by precipitation [60]. Our study revealed a nonlinear relationship between rainfall and the growth rate of poplar trees. With increasing rainfall, the growth rate of poplar trees in the small diameter class tends to increase, albeit with erratic fluctuations. Moderate to moderately high rainfall environments result in higher growth rates for poplar trees in the medium-diameter class, although they are still subjected to fluctuations caused by other factors. Conversely, in high rainfall environments, the growth rate of poplar trees in the large diameter class decreases. In a study [61], a positive correlation was found between tree growth and rainfall in tropical regions. However, in our study, we observed differences in the response of poplar tree growth rates among different diameter classes as rainfall increased. This variation may be attributed to differences in water use efficiency among poplar trees of various sizes. Poplar trees in the small diameter class exhibit lower water use efficiency and are more vulnerable to inadequate rainfall. Poplar trees in the medium diameter class respond more significantly to rainfall compared to those in the small diameter class, owing to their thicker trunk and well-established root system. The growth rate of poplar trees in the large diameter class appears to be less responsive to rainfall, potentially due to factors like root hypoxia or root decay arising from excessive moisture in such conditions. Additionally, future research should emphasize the impact of rainfall on soil moisture and the water absorption capability of tree roots in soils with varying thicknesses—areas that are worthy of investigation [62–65]. However, our study did not extensively delve into these particular aspects.

The growth of poplar trees is negatively correlated with elevation. The humidity and thermal conditions generally change with variations in the elevation of mountain slopes [66]. Poplar trees in the small diameter class exhibit higher growth rates in lower elevation environments, possibly due to favorable factors like increased temperatures and fertile soil. With the increase of elevation, the environment progressively worsens, resulting in a gradual decrease in the growth rate of poplar trees in the small diameter class. The impact of elevation on the growth rate of poplar trees in the medium diameter class is not significant in low, low-moderate, moderate, and moderate-high elevation environments, with only a slight decrease. This is because medium-diameter poplar trees have strong growth capabilities and can adapt to a broader range of environmental conditions. In high-elevation environments, the influences of factors such as temperature and lighting are more noticeable, leading to a considerable decrease in the growth rate of medium-diameter poplar trees. In lower-elevation environments, larger-diameter poplar trees require more resources to maintain growth, resulting in greater fluctuations in the growth rate. The response of large-diameter poplar trees to changes in elevation gradients is not significantly different. Variations in tree growth patterns among different tree species and elevations can be attributed to plant physiological traits [66]. Nevertheless, this characteristic of poplar trees corresponds to the findings of [50] in their study of fir forests.

Generally, the growth of poplar trees of different sizes has been promoted with the increase in temperature. In cold regions, the growth rate of poplar trees exhibits an inverted 'J' curve with increasing breast diameter. Initially, the growth rate is high, gradually decreasing with increased breast diameter. While poplar trees in the small diameter class exhibit strong growth capacity and maintain a higher growth rate, those in the medium and large diameter classes have relatively lower growth rates. With increasing temperature, the growth rate of poplar trees in all three diameter classes generally increases but becomes more fluctuating. This is due to the impact of temperature changes on growth factors such as photosynthesis, water evaporation, and nutrient absorption in trees [67]. Notably,

in the transition from moderate to high-temperature environments, the growth rate of poplar trees in the small diameter class decreases. This could be attributed to reduced soil moisture and weaker root systems, which result in lower water absorption efficiency and water deprivation under high-temperature conditions [60,68,69]. Morales et al. [60] found a negative correlation between temperature and radial growth in their study. However, the analysis of nationwide sample data in this study indicates that the growth of poplar is generally promoted by increasing temperature. These differences can be attributed to the fact that although certain regions in the study experience high temperatures, they receive sufficient rainfall within the appropriate range for poplar growth. Other studies [68,70] have shown that high annual temperatures have a strong negative impact on radial growth in trees. Conversely, variations in the lowest annual temperature have minimal impacts on tree growth. Therefore, when cultivating poplar groves, it is essential to consider local climate characteristics and implement appropriate protective and management measures to mitigate the impact of extreme temperature events.

Additionally, in analyzing the distribution of growth rates among poplar trees of varying sizes in relation to different forest stand densities, levels of rainfall, altitudes, and temperatures, it was observed that at low forest stand density levels, the Height Diameter Deviation Angle (HDDA) of poplar trees with a size range of 7.5–20 cm exhibited a growth rate ranging from 0.5 to 0.15. As the forest stand density increased, the HDDA of poplar trees consistently declined within the size and growth rate range, ultimately remaining in the size range of 5–10 cm with a growth rate of 0–0.1. The influence of varying rainfall levels on HDDA indicated that as rainfall increased, there was a shift in the size range of poplar trees from 7.5–17.5 cm with a growth rate of 0.5–1.25 to 7.5–12.5 cm with a growth rate of 0.25–0.5, and further to 7.5–15 cm with a growth rate of 0.25–1.5. As the altitude increased, the HDDA of poplar trees also decreased, settling in the low size and low growth rate range of 5–10 cm with a growth rate of 0–0.5. In cold temperature environments, the HDDA of poplar trees was distributed in the size range of 5–15 cm with a growth rate of 0–0.1. As the temperature increased, the HDDA progressively decreased, suggesting that higher temperatures increased the variability in the growth rate of poplar trees of various sizes, resulting in a more even distribution between low-growth-rate and high-growth-rate poplar trees of different sizes. The variations in the distribution of HDDA among poplar trees across different environmental conditions indicate the adaptability and growth characteristics of poplar trees in diverse environmental settings.

Poplar trees can benefit from increased resource availability in environments characterized by low forest stand density, high rainfall, low altitude, and high temperature. Conversely, in environments with high forest stand density, moderate rainfall, high altitude, and low temperature, the growth of poplar trees is impeded. To mitigate the effects of these varying environmental conditions, the following strategies can be implemented for the establishment and management of poplar plantations: In regions characterized by high forest stand density, tree density can be regulated through thinning practices to alleviate competitive resource interactions among individual trees; In regions experiencing low rainfall and high temperature, it is crucial to enhance irrigation practices to ensure an adequate water supply for the growth of poplar trees; In high-altitude regions, emphasis should be placed on selecting locally adapted poplar varieties, alongside implementing ecological restoration and vegetation protection measures to sustain equilibrium and stability within the local ecosystem; In cold regions, it is essential to enhance protective measures, including the utilization of covering materials or insulation, to safeguard poplar seedlings and delicate branches from frost damage. In summary, implementing appropriate planting and protection measures tailored to the impact of various environmental factors can effectively enhance the growth and ecological benefits of poplar plantations.

## 5. Conclusions

This study aimed to predict the growth rate of poplar trees using various models, and the results showed that the DNN-RF integrated model had the highest accuracy, with

$R^2$ , MAE, and RMSE values of 0.893, 1.958%, and 2.844%, respectively. Furthermore, we observed fluctuations in the growth rate of poplar trees of various sizes under the influence of different levels of stand density, rainfall, altitude, and temperature. Under conditions of low stand density, high rainfall, low altitude, and high temperature, the growth rate of poplar trees considerably increased, particularly among larger individuals displaying heightened growth rates. Conversely, in environments characterized by high stand density, moderate rainfall, high altitude, and low temperature, the growth of poplar trees was constrained. Thus, it is important to consider factors such as stand density, rainfall, altitude, and temperature when studying the growth of poplar trees. While this study successfully identified the key factors that influence the growth rate of poplar trees, it primarily focused on analyzing individual features and their impact on the growth rate of poplar trees at various sizes without exploring the mechanisms underlying the combined effects of multiple features on growth rates. Therefore, future research should delve deeper into examining the influence of multiple features on the growth rate of poplar trees.

**Author Contributions:** B.Z., Z.F. and G.L. conceived and designed the study; Z.F. and B.Z. collected the data; B.Z., G.L., M.Z. and T.M. processed the data; B.Z., M.Z. and X.Z. (Xin Zhao) performed the model fitting; B.Z., X.Z. (Xiaoyuan Zhang) and Z.S. supported data analysis; and B.Z. and M.Z. wrote the main manuscript. All authors contributed to writing and reviewing the paper. All authors have read and agreed to the published version of the manuscript.

**Funding:** This study was supported by the Natural Science Foundation of Beijing (8232038, 8234065) and the Key Research and Development Projects of Ningxia Hui Autonomous Region (2023BEG02050).

**Data Availability Statement:** Not applicable.

**Acknowledgments:** The authors sincerely thank the editors and the anonymous reviewers for their constructive feedback.

**Conflicts of Interest:** The authors declare no conflict of interest.

## References

1. Dong, S.; Wang, Z. Study on the geographic distribution pattern of *Populus* in China. *Chin. J. Ecol.* **1988**, *7*, 12–18. [[CrossRef](#)]
2. Zeng, W.; Chen, X.; Yang, X. Biomass Modeling and Productivity Analysis of Planted *Populus* spp. in China. *Sci. Silvae Sin.* **2019**, *55*, 1–8. [[CrossRef](#)]
3. National Forestry and Grassland Administration. *China Forest Resources Reported (2014–2018)*; China Forestry Publishing House: Beijing, China, 2019.
4. Pan, Y. *Study on Some Major Issues of the Fifth Phase of the Three-North Protective Forest System Construction Project*; Ningxia Sunshine Publishing House: Ningxia, China, 2013.
5. Liu, Y.; Xin, Z.; Li, Z.; Keyimu, M. Climate effect on the radial growth of *Populus simonii* in Northwest of Hebei for last four decades. *Acta Ecol. Sin.* **2020**, *40*, 9108–9119. [[CrossRef](#)]
6. Pinard, M.; Howlett, B.; Davidson, D. Site Conditions Limit Pioneer Tree Recruitment After Logging of Dipterocarp Forests in Sabah, Malaysia. *Biotropica* **1996**, *28*, 2. [[CrossRef](#)]
7. Huang, X.; Dai, D.; Xiang, Y.; Yan, Z.; Teng, M.; Wang, P.; Zhou, Z.; Zeng, L.; Xiao, W. Radial Growth of *Pinus Massoniana* Is Influenced by Temperature, Precipitation, and Site Conditions on the Regional Scale: A Meta-Analysis Based on Tree-Ring Width Index. *Ecol. Indic.* **2021**, *126*, 107659. [[CrossRef](#)]
8. Mérian, P.; Lebourgeois, F. Size-Mediated Climate–Growth Relationships in Temperate Forests: A Multi-Species Analysis. *For. Ecol. Manag.* **2011**, *261*, 1382–1391. [[CrossRef](#)]
9. Copenheaver, C.A.; Crawford, C.J.; Fearer, T.M. Age-Specific Responses to Climate Identified in the Growth of *Quercus Alba*. *Trees* **2011**, *25*, 647–653. [[CrossRef](#)]
10. Linares, J.C.; Camarero, J.J.; Carreira, J.A. Competition Modulates the Adaptation Capacity of Forests to Climatic Stress: Insights from Recent Growth Decline and Death in Relict Stands of the Mediterranean Fir *Abies Pinsapo*. *J. Ecol.* **2010**, *98*, 592–603. [[CrossRef](#)]
11. D’Amato, A.W.; Bradford, J.B.; Fraver, S.; Palik, B.J. Effects of Thinning on Drought Vulnerability and Climate Response in North Temperate Forest Ecosystems. *Ecol. Appl.* **2013**, *23*, 1735–1742. [[CrossRef](#)] [[PubMed](#)]
12. Kolb, T.E.; Steiner, K.C.; McCormick, L.H.; Bowersox, T.W. Growth Response of Northern Red-Oak and Yellow-Poplar Seedlings to Light, Soil Moisture and Nutrients in Relation to Ecological Strategy. *For. Ecol. Manag.* **1990**, *38*, 65–78. [[CrossRef](#)]
13. Radojčić Redovniković, I.; De Marco, A.; Proietti, C.; Hanousek, K.; Sedak, M.; Bilandžić, N.; Jakovljević, T. Poplar Response to Cadmium and Lead Soil Contamination. *Ecotoxicol. Environ. Saf.* **2017**, *144*, 482–489. [[CrossRef](#)]

14. Feeley, K.J.; Joseph Wright, S.; Nur Supardi, M.N.; Kassim, A.R.; Davies, S.J. Decelerating Growth in Tropical Forest Trees. *Ecol. Lett.* **2007**, *10*, 461–469. [[CrossRef](#)] [[PubMed](#)]
15. Centritto, M.; Brillì, F.; Fodale, R.; Loreto, F. Different Sensitivity of Isoprene Emission, Respiration and Photosynthesis to High Growth Temperature Coupled with Drought Stress in Black Poplar (*Populus nigra*) Saplings. *Tree Physiol.* **2011**, *31*, 275–286. [[CrossRef](#)] [[PubMed](#)]
16. LeBlanc, D.; Maxwell, J.; Pederson, N.; Berland, A.; Mandra, T. Radial Growth Responses of Tulip Poplar (*Liriodendron tulipifera*) to Climate in the Eastern United States. *Ecosphere* **2020**, *11*, e03203. [[CrossRef](#)]
17. Yao, Y.; Shu, S.; Wang, W.; Liu, R.; Wang, Y.; Wang, X.; Zhang, S. Growth and Carbon Sequestration of Poplar Plantations on the Tibetan Plateau. *Ecol. Indic.* **2023**, *147*, 109930. [[CrossRef](#)]
18. Fernández-de-Uña, L.; McDowell, N.G.; Cañellas, I.; Gea-Izquierdo, G. Disentangling the Effect of Competition, CO<sub>2</sub> and Climate on Intrinsic Water-Use Efficiency and Tree Growth. *J. Ecol.* **2016**, *104*, 678–690. [[CrossRef](#)]
19. Wang, D.; Fan, J.; Jing, P.; Cheng, Y.; Ruan, H. Analyzing the Impact of Climate and Management Factors on the Productivity and Soil Carbon Sequestration of Poplar Plantations. *Environ. Res.* **2016**, *144*, 88–95. [[CrossRef](#)] [[PubMed](#)]
20. Xue, X.; Jin, S.; An, F.; Zhang, H.; Fan, J.; Eichhorn, M.P.; Jin, C.; Chen, B.; Jiang, L.; Yun, T. Shortwave Radiation Calculation for Forest Plots Using Airborne LiDAR Data and Computer Graphics. *Plant Phenomics* **2022**, *2022*, 9856739. [[CrossRef](#)] [[PubMed](#)]
21. Peng, C. Growth and Yield Models for Uneven-Aged Stands: Past, Present and Future. *For. Ecol. Manag.* **2000**, *132*, 259–279. [[CrossRef](#)]
22. Porté, A.; Bartelink, H.H. Modelling Mixed Forest Growth: A Review of Models for Forest Management. *Ecol. Model.* **2002**, *150*, 141–188. [[CrossRef](#)]
23. Ashraf, M.I.; Zhao, Z.; Bourque, C.P.-A.; MacLean, D.A.; Meng, F.-R. Integrating Biophysical Controls in Forest Growth and Yield Predictions with Artificial Intelligence Technology. *Can. J. For. Res.* **2013**, *43*, 1162–1171. [[CrossRef](#)]
24. Fox, J.C.; Ades, P.K.; Bi, H. Stochastic Structure and Individual-Tree Growth Models. *For. Ecol. Manag.* **2001**, *154*, 261–276. [[CrossRef](#)]
25. Guo, C.; Guo, H.; Wang, B. Study on increment model of individual-tree diameter of *Cunninghamia lanceolata* in consideration of climatic factors. *J. Nanjing For. Univ. (Nat. Sci. Ed.)* **2023**, *47*, 47–56. [[CrossRef](#)]
26. Zhang, H.; Feng, Z.; Huang, G.; Yang, X.; Feng, Z. Research on the growth rate model of *Populus* spp. considering environmental factors. *J. Beijing For. Univ.* **2022**, *44*, 50–59. [[CrossRef](#)]
27. Yang, X.; Wang, J.; Du, Z.; Wang, W.; Meng, J. Development of individual-tree diameter increment model for natural *Larix gmelinii* forests based on climatic factors. *J. Beijing For. Univ.* **2022**, *44*, 1–11. [[CrossRef](#)]
28. Bodesheim, P.; Babst, F.; Frank, D.C.; Hartl, C.; Zang, C.S.; Jung, M.; Reichstein, M.; Mahecha, M.D. Predicting Spatiotemporal Variability in Radial Tree Growth at the Continental Scale with Machine Learning. *Environ. Data Sci.* **2022**, *1*, e9. [[CrossRef](#)]
29. Wang, Z.; Zhang, X.; Zhang, J.; Chhin, S. Effects of Stand Factors on Tree Growth of Chinese Fir in the Subtropics of China Depends on Climate Conditions from Predictions of a Deep Learning Algorithm: A Long-Term Spacing Trial. *For. Ecol. Manag.* **2022**, *520*, 120363. [[CrossRef](#)]
30. Healey, S.P.; Cohen, W.B.; Yang, Z.; Kenneth Brewer, C.; Brooks, E.B.; Gorelick, N.; Hernandez, A.J.; Huang, C.; Joseph Hughes, M.; Kennedy, R.E.; et al. Mapping Forest Change Using Stacked Generalization: An Ensemble Approach. *Remote Sens. Environ.* **2018**, *204*, 717–728. [[CrossRef](#)]
31. Saha, S.; Saha, M.; Mukherjee, K.; Arabameri, A.; Ngo, P.T.T.; Paul, G.C. Predicting the Deforestation Probability Using the Binary Logistic Regression, Random Forest, Ensemble Rotational Forest, REPTree: A Case Study at the Gumani River Basin, India. *Sci. Total Environ.* **2020**, *730*, 139197. [[CrossRef](#)] [[PubMed](#)]
32. Wang, T.; Wang, G.; Innes, J.L.; Seely, B.; Chen, B. ClimateAP: An Application for Dynamic Local Downscaling of Historical and Future Climate Data in Asia Pacific. *Front. Agric. Sci. Eng.* **2017**, *4*, 448. [[CrossRef](#)]
33. Wang, B.; Wei, W.; Xing, Z.; You, W.; Niu, X.; Ren, X.; Liu, C. Biomass Carbon Pools of *Cunninghamia lanceolata* (Lamb.) Hook. Forests in Subtropical China: Characteristics and Potential. *Scand. J. For. Res.* **2012**, *27*, 545–560. [[CrossRef](#)]
34. Wang, T.; Hamann, A.; Spittlehouse, D.L.; Murdock, T.Q. ClimateWNA—High-Resolution Spatial Climate Data for Western North America. *J. Appl. Meteorol. Climatol.* **2012**, *51*, 16–29. [[CrossRef](#)]
35. Zhang, H.; Feng, Z.; Shen, C.; Li, Y.; Feng, Z.; Zeng, W.; Huang, G. Relationship between the Geographical Environment and the Forest Carbon Sink Capacity in China Based on an Individual-Tree Growth-Rate Model. *Ecol. Indic.* **2022**, *138*, 108814. [[CrossRef](#)]
36. Su, X.; Yan, X.; Tsai, C.-L. Linear Regression: Linear Regression. *WIREs Comp. Stat.* **2012**, *4*, 275–294. [[CrossRef](#)]
37. Murtagh, F. Multilayer Perceptrons for Classification and Regression. *Neurocomputing* **1991**, *2*, 183–197. [[CrossRef](#)]
38. Franco-Lopez, H.; Ek, A.R.; Bauer, M.E. Estimation and Mapping of Forest Stand Density, Volume, and Cover Type Using the k-Nearest Neighbors Method. *Remote Sens. Environ.* **2001**, *77*, 251–274. [[CrossRef](#)]
39. Keramat-Jahromi, M.; Mohtasebi, S.S.; Mousazadeh, H.; Ghasemi-Varnamkhasti, M.; Rahimi-Movassagh, M. Real-Time Moisture Ratio Study of Drying Date Fruit Chips Based on on-Line Image Attributes Using KNN and Random Forest Regression Methods. *Measurement* **2021**, *172*, 108899. [[CrossRef](#)]
40. Cheshmberah, F.; Fathizad, H.; Parad, G.A.; Shojaeifar, S. Comparison of RBF and MLP Neural Network Performance and Regression Analysis to Estimate Carbon Sequestration. *Int. J. Environ. Sci. Technol.* **2020**, *17*, 3891–3900. [[CrossRef](#)]
41. Breiman, L. Random Forests. *Mach. Learn.* **2001**, *45*, 5–32. [[CrossRef](#)]
42. Liaw, A.; Wiener, M. Classification and Regression by RandomForest. *R News* **2002**, *2*, 18–22.

43. Jeong, S.; Ko, J.; Shin, T.; Yeom, J. Incorporation of Machine Learning and Deep Neural Network Approaches into a Remote Sensing-Integrated Crop Model for the Simulation of Rice Growth. *Sci. Rep.* **2022**, *12*, 9030. [[CrossRef](#)]
44. Pedregosa, F.; Varoquaux, G.; Gramfort, A.; Michel, V.; Thirion, B.; Grisel, O.; Blondel, M.; Prettenhofer, P.; Weiss, R.; Dubourg, V.; et al. Scikit-learn: Machine learning in Python. *J. Mach. Learn. Res.* **2011**, *12*, 2825–2830.
45. Agrawal, T. Hyperparameter Optimization Using Scikit-Learn. In *Hyperparameter Optimization in Machine Learning*; Apress: Berkeley, CA, USA, 2021; pp. 31–51, ISBN 978-1-4842-6578-9.
46. Altmann, A.; Tološi, L.; Sander, O.; Lengauer, T. Permutation Importance: A Corrected Feature Importance Measure. *Bioinformatics* **2010**, *26*, 1340–1347. [[CrossRef](#)] [[PubMed](#)]
47. Eby, W.M.; Oyamakin, S.O.; Chukwu, A.U. A New Nonlinear Model Applied to the Height-DBH Relationship in Gmelina Arborea. *For. Ecol. Manag.* **2017**, *397*, 139–149. [[CrossRef](#)]
48. McLaughlin, S.B.; Wullschleger, S.D.; Nosal, M. Diurnal and Seasonal Changes in Stem Increment and Water Use by Yellow Poplar Trees in Response to Environmental Stress. *Tree Physiol.* **2003**, *23*, 1125–1136. [[CrossRef](#)] [[PubMed](#)]
49. Liang, Z.-S.; Yang, J.-W.; Shao, H.-B.; Han, R.-L. Investigation on Water Consumption Characteristics and Water Use Efficiency of Poplar under Soil Water Deficits on the Loess Plateau. *Colloids Surf. B Biointerfaces* **2006**, *53*, 23–28. [[CrossRef](#)] [[PubMed](#)]
50. Primicia, I.; Camarero, J.J.; Janda, P.; Čada, V.; Morrissey, R.C.; Trotsiuk, V.; Bače, R.; Teodosiu, M.; Svoboda, M. Age, Competition, Disturbance and Elevation Effects on Tree and Stand Growth Response of Primary Picea Abies Forest to Climate. *For. Ecol. Manag.* **2015**, *354*, 77–86. [[CrossRef](#)]
51. Zhu, Y.; Li, D.; Fan, J.; Zhang, H.; Eichhorn, M.P.; Wang, X.; Yun, T. A Reinterpretation of the Gap Fraction of Tree Crowns from the Perspectives of Computer Graphics and Porous Media Theory. *Front. Plant Sci.* **2023**, *14*, 1109443. [[CrossRef](#)]
52. Larocque, G.R. Performance and Morphological Response of the Hybrid Poplar DN-74 (*Populus Deltoides* × *Nigra*) under Different Spacings on a 4-Year Rotation. *Ann. For. Sci.* **1999**, *56*, 275–287. [[CrossRef](#)]
53. Waring, R.H. Characteristics of Trees Predisposed to Die. *BioScience* **1987**, *37*, 569–574. [[CrossRef](#)]
54. Shi, H.; Zhang, L. Local Analysis of Tree Competition and Growth. *For. Sci.* **2003**, *49*, 938–955. [[CrossRef](#)]
55. Latham, P.; Tappeiner, J. Response of Old-Growth Conifers to Reduction in Stand Density in Western Oregon Forests. *Tree Physiol.* **2002**, *22*, 137–146. [[CrossRef](#)]
56. Hurteau, M.D.; Brooks, M.L. Short- and Long-Term Effects of Fire on Carbon in US Dry Temperate Forest Systems. *BioScience* **2011**, *61*, 139–146. [[CrossRef](#)]
57. Kerhoulas, L.P.; Kolb, T.E.; Hurteau, M.D.; Koch, G.W. Managing Climate Change Adaptation in Forests: A Case Study from the U.S. Southwest. *J. Appl. Ecol.* **2013**, *50*, 1311–1320. [[CrossRef](#)]
58. Hurteau, M.D.; Stoddard, M.T.; Fulé, P.Z. The Carbon Costs of Mitigating High-Severity Wildfire in Southwestern Ponderosa Pine: CARBON COSTS OF MITIGATING WILDFIRE. *Glob. Chang. Biol.* **2011**, *17*, 1516–1521. [[CrossRef](#)]
59. Plauborg, K.U. Analysis of Radial Growth Responses to Changes in Stand Density for Four Tree Species. *For. Ecol. Manag.* **2004**, *188*, 65–75. [[CrossRef](#)]
60. Morales, M.S.; Villalba, R.; Grau, H.R.; Paolini, L. Rainfall-Controlled Tree Growth in High-Elevation Subtropical Treelines. *Ecology* **2004**, *85*, 3080–3089. [[CrossRef](#)]
61. Brienen, R.J.W.; Zuidema, P.A. Relating Tree Growth to Rainfall in Bolivian Rain Forests: A Test for Six Species Using Tree Ring Analysis. *Oecologia* **2005**, *146*, 1–12. [[CrossRef](#)]
62. Aa, Y.; Wang, G.; Sun, W.; Xue, B.; Kiem, A. Stratification Response of Soil Water Content during Rainfall Events under Different Rainfall Patterns. *Hydrol. Process.* **2018**, *32*, 3128–3139. [[CrossRef](#)]
63. Romero-Saltos, H.; Sternberg, L.D.S.L.; Moreira, M.Z.; Nepstad, D.C. Rainfall Exclusion in an Eastern Amazonian Forest Alters Soil Water Movement and Depth of Water Uptake. *Am. J. Bot.* **2005**, *92*, 443–455. [[CrossRef](#)]
64. Wilson, K.B.; Hanson, P.J.; Mulholland, P.J.; Baldocchi, D.D.; Wullschleger, S.D. A Comparison of Methods for Determining Forest Evapotranspiration and Its Components: Sap-Flow, Soil Water Budget, Eddy Covariance and Catchment Water Balance. *Agric. For. Meteorol.* **2001**, *106*, 153–168. [[CrossRef](#)]
65. Clausnitzer, F.; Köstner, B.; Schwärzel, K.; Bernhofer, C. Relationships between Canopy Transpiration, Atmospheric Conditions and Soil Water Availability—Analyses of Long-Term Sap-Flow Measurements in an Old Norway Spruce Forest at the Ore Mountains/Germany. *Agric. For. Meteorol.* **2011**, *151*, 1023–1034. [[CrossRef](#)]
66. Gao, L.; Gou, X.; Deng, Y.; Yang, M.; Zhang, F. Assessing the Influences of Tree Species, Elevation and Climate on Tree-Ring Growth in the Qilian Mountains of Northwest China. *Trees* **2017**, *31*, 393–404. [[CrossRef](#)]
67. Solberg, S.; Dobbertin, M.; Reinds, G.J.; Lange, H.; Andreassen, K.; Fernandez, P.G.; Hildingsson, A.; De Vries, W. Analyses of the Impact of Changes in Atmospheric Deposition and Climate on Forest Growth in European Monitoring Plots: A Stand Growth Approach. *For. Ecol. Manag.* **2009**, *258*, 1735–1750. [[CrossRef](#)]
68. Schippers, P.; Sterck, F.; Vlam, M.; Zuidema, P.A. Tree Growth Variation in the Tropical Forest: Understanding Effects of Temperature, Rainfall and CO<sub>2</sub>. *Glob. Chang. Biol.* **2015**, *21*, 2749–2761. [[CrossRef](#)]

- 
69. Hatfield, J.L.; Dold, C. Water-Use Efficiency: Advances and Challenges in a Changing Climate. *Front. Plant Sci.* **2019**, *10*, 103. [[CrossRef](#)]
  70. Vlam, M.; Baker, P.J.; Bunyavejchewin, S.; Zuidema, P.A. Temperature and Rainfall Strongly Drive Temporal Growth Variation in Asian Tropical Forest Trees. *Oecologia* **2014**, *174*, 1449–1461. [[CrossRef](#)]

**Disclaimer/Publisher’s Note:** The statements, opinions and data contained in all publications are solely those of the individual author(s) and contributor(s) and not of MDPI and/or the editor(s). MDPI and/or the editor(s) disclaim responsibility for any injury to people or property resulting from any ideas, methods, instructions or products referred to in the content.